Gradient-Based Predictive Pulse Pattern Control for Medium-Voltage Drives with Very Fast Transients

Ilari Hilden
Faculty of Inf. Technol. and Commun. Sciences
Tampere University
Tampere, Finland
ilari.hilden@tuni.fi

Petros Karamanakos
Faculty of Inf. Technol. and Commun. Sciences
Tampere University
Tampere, Finland
p.karamanakos@ieee.org

Tobias Geyer
Motion System Drives
ABB Switzerland Ltd
Turgi, Switzerland
t.geyer@ieee.org

***Abstract*—Gradient-based predictive pulse pattern control (GP^{3}C) is a versatile optimal control method for medium-voltage (MV) drives. GP^{3}C combines model predictive control (MPC) and optimized pulse patterns (OPPs) to achieve superb steady-state performance. The rigid nature of OPPs, however, can compromise its dynamic behavior. To address this, this paper augments GP^{3}C with a mechanism that enables the full utilization of the available voltage, and thus very short settling times.**

***Index Terms*—Medium-voltage (MV) drive, model predictive control (MPC), optimized pulse patterns (OPPs)**

I. Introduction

Medium-voltage (MV) drives are operated at switching frequencies of a few hundred hertz to keep the switching losses low [1]. Operating the converter at such low switching frequencies gives rise to pronounced stator current distortions. To mitigate this, optimized pulse patterns (OPPs) can be used as they produce the lowest possible harmonic distortions [2].

Manipulation of OPPs with a high-bandwidth controller, however, is a nontrivial task. This can be addressed by using model predictive control (MPC) [3], see [4]. Recently, a highly versatile MPC strategy that manipulates OPPs in real time—referred to as gradient-based predictive pulse pattern control (GP^{3}C)—was presented in [5]. The GP^{3}C algorithm can outperform conventional linear control strategies [6] by utilizing both the high bandwidth of direct MPC [7], [8], and the excellent steady-state performance of OPPs [9]. However, the rigid nature of OPPs results in limited options in the available switch positions that can be manipulated [10]. This implies that the available voltage margin of the converter can be underutilized, compromising the dynamic performance.

To resolve this issue, this work complements the GP^{3}C algorithm by introducing a strategy to locally overwrite the OPP during transients. As a result, the available voltage margin is fully utilized, and superior dynamic performance is achieved. The comparisons with finite control set MPC (FCS-MPC) [11]—which is known to achieve the shortest possible settling times—based on a three-level neutral-point-clamped (NPC) converter and an MV induction machine (IM) demonstrate the effectiveness of the proposed strategy.

II. GP^{3}C for MV Drives with Pulse Insertion

The GP^{3}C algorithm in [5] manipulates all three phases of the OPP simultaneously such that the stator current follows its optimal trajectory [12].[1] Nevertheless, GP^{3}C is limited to using only these three-phase switch positions that are present in the OPP in a fixed chronological order. Therefore, the switch positions that can quickly drive the stator current to its reference are not always available when substantial modifications to the nominal OPP are required, e.g., during transients. To address this, and guarantee that the available voltage margin is fully utilized, the OPP is *locally* overwritten with three-phase switch positions that do not exist in the nominal OPP when the torque error exceeds a predefined limit.

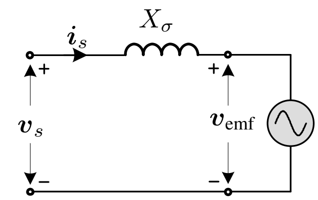

Fig. 1. Equivalent circuit of an MV IM.

To this end, the simplified equivalent circuit of an MV IM is considered [13], see Fig. 1. By neglecting the stator resistance—which is typically very small in MV machines—the dynamics of the system in question are described by

$$\frac{\mathrm{d}\boldsymbol{i}_s}{\mathrm{d}t} = \frac{1}{X_\sigma}(\boldsymbol{v}_s - \boldsymbol{v}_{\text{emf}})\,, \tag{1}$$

where $\boldsymbol{i}_s$ and $\boldsymbol{v}_s$ are the stator current and voltage, respectively, and $\boldsymbol{v}_{\text{emf}}$ is the back electromotive force (back-EMF) of the machine.[2] Finally, X_σ is the total leakage reactance.

From (1) it can be deduced that the change in the stator current within one sampling interval T_s is

$$\Delta\boldsymbol{i}_s = \frac{T_s}{X_\sigma}(\boldsymbol{v}_s - \boldsymbol{v}_{\text{emf}})\,.$$

Therefore, for fast torque control, the stator current error should quickly converge to zero, implying $\Delta\boldsymbol{i}_s = \boldsymbol{i}_{s,\text{ref}} - \boldsymbol{i}_s \to 0$, where $\boldsymbol{i}_{s,\text{ref}}$ is the stator current reference. As a result, the voltage $\boldsymbol{v}_{s,\text{ideal}}$ required by the converter to achieve this is

$$\boldsymbol{v}_{s,\text{ideal}} = \frac{X_\sigma}{T_s}(\boldsymbol{i}_{s,\text{ref}} - \boldsymbol{i}_s) + \boldsymbol{v}_{\text{emf}}\,.$$

[1] For a detailed presentation of the GP^{3}C algorithm and the MV drive system, the reader is referred to [5].

[2] Note that all variables are in the $\alpha\beta$ reference frame.

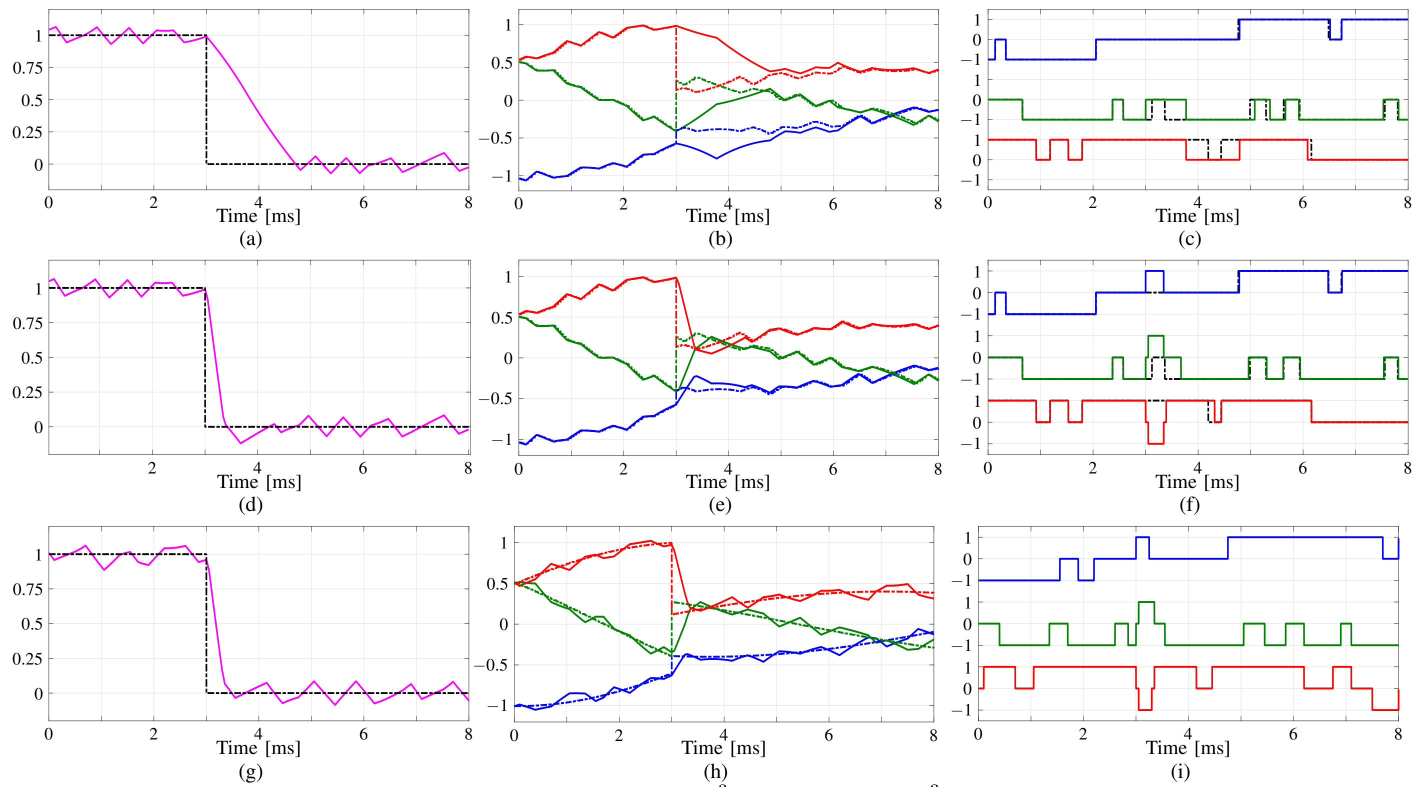

Fig. 2. Simulation results (in per unit) during a torque reference step for GP^{3}C from [5] (a)–(c), GP^{3}C with pulse insertion (d)–(e), and FCS-MPC (g)–(i): (a), (d), (g) Electromagnetic torque (solid line) and its reference (dash-dotted line); (b), (e), (h) three-phase stator current (solid lines) and their references (dash-dotted lines); (c), (f) three-phase (modified) switching pattern (solid lines) and nominal OPP (dash-dotted lines); (i) three-phase switching pattern.

However, because the three-level NPC converter can only produce 27 discrete voltage vectors (i.e., three-phase switch positions) $\boldsymbol{v}_i$, $i \in \{1, 2, \dots, 27\}$, the realizable converter voltage vector is

$$\boldsymbol{v}_{s,\text{ins}} = \min\left(\|\boldsymbol{v}_i - \boldsymbol{v}_{s,\text{ideal}}\|_2\right) , \quad i \in \{1, 2, \dots, 27\} . \tag{2}$$

Hence, by translating $\boldsymbol{v}_{s,\text{ins}}$ into a three-phase switch position, and by inserting the latter into the OPP, shorter settling times can be achieved during a torque transient.

Once the to-be-inserted three-phase switch position has been determined, the next step is to decide where to locally overwrite the OPP. This is done by exploiting the predictive nature of GP^{3}C such that the additional three-phase switch positions are dynamically inserted within the prediction horizon. To this end, the current prediction at the previous time step $k-1$, $k \in \mathbb{N}^+$, is utilized to determine if the magnitude of the stator current error convergences monotonically to zero within the horizon. Specifically, the predicted current trajectory at $k-1$ is scanned with $T_c \ll T_s$ to monitor the evolution of the current error magnitude $i_{s,\text{err}} = \|\boldsymbol{i}_{s,\text{ref}} - \boldsymbol{i}_s\|_2$ at the discrete time steps $p \in \mathbb{N}^+$, i.e.,

$$\boldsymbol{I}_{s,\text{err}}(k-1) = \begin{bmatrix} i_{s,\text{err}}(p) & i_{s,\text{err}}(p+1) & \dots & i_{s,\text{err}}(p+m) \end{bmatrix}^T ,$$

where $m = (N_p - 1)T_s/T_c$, with N_p being the number of prediction steps. For the stator current error to be decreasing, the difference between every two consecutive entries of $\boldsymbol{I}_{s,\text{err}}$ must be negative, i.e.,

$$i_{s,\text{err}}(p+\ell) - i_{s,\text{err}}(p+\ell-1) < 0 , \quad \ell \in \{1, 2, \dots, m\} . \tag{3}$$

Therefore, the first time instant $t_{\text{ins}} = kT_s + \ell T_c$ in the prediction horizon where condition (3) is violated the chosen three-phase switch position (see (2)) is inserted into the OPP as a pulse of infinitesimal width. This pulse is freely manipulated by GP^{3}C to eliminate the current error. Note that if condition (3) is not violated for any ℓ, a pulse insertion is not performed.

III. Performance Evaluation

Fig. 2 compares the dynamic performance of GP^{3}C from [5], GP^{3}C with the proposed pulse insertion mechanism, and FCS-MPC [11] based on an MV drive system. The parameters of the system and GP^{3}C can be found in [5]. Both GP^{3}C and FCS-MPC use $T_s = 50\,\mu$s and operate at a switching frequency of 250 Hz. As can be seen from Figs. 2(a) and 2(d), thanks to the proposed pulse insertion algorithm the settling time of GP^{3}C improves by more than 75% compared with GP^{3}C in [5], while it is comparable to FCS-MPC, see Fig. 2(g). This is achieved by manipulating the three-phase switch position $\boldsymbol{u}_{abc} = [1\ 1\ -1]^T$, inserted at around $t = 3$ ms, see Fig. 2(f).

IV. Conclusion

This work improved the dynamic performance of the GP^{3}C algorithm for MV drives presented in [5]. To achieve this, a pulse insertion algorithm was proposed that enables the full utilization of the available voltage margin during transients. As a result, the settling time of GP^{3}C is improved by more than 75%, while it is on par with that of FCS-MPC.

Acknowledgment

This work was supported by the Research Council of Finland.

References

[1] J. Rodríguez, S. Bernet, B. Wu, J. O. Pontt, and S. Kouro, “Multilevel voltage-source-converter topologies for industrial medium-voltage drives,” *IEEE Trans. Ind. Electron.*, vol. 54, no. 6, pp. 2930–2945, Dec. 2007.

[2] G. S. Buja and G. B. Indri, “Optimal pulsewidth modulation for feeding ac motors,” *IEEE Trans. Ind. Appl.*, vol. IA-13, no. 1, pp. 38–44, Jan./Feb. 1977.

[3] J. B. Rawlings and D. Q. Mayne, *Model Predictive Control: Theory and Design*. Madison, WI: Nob Hill, 2009.

[4] T. Geyer, N. Oikonomou, G. Papafotiou, and F. D. Kieferndorf, “Model predictive pulse pattern control,” *IEEE Trans. Ind. Appl.*, vol. 48, no. 2, pp. 663–676, Mar./Apr. 2012.

[5] M. A. W. Begh, P. Karamanakos, and T. Geyer, “Gradient-based predictive pulse pattern control of medium-voltage drives—Part I: Control, concept, and analysis,” *IEEE Trans. Power Electron.*, vol. 37, no. 12, pp. 14 222–14 236, Dec. 2022.

[6] M. A. W. Begh, P. Karamanakos, T. Geyer, and Q. Yang, “Gradient-based predictive pulse pattern control of medium-voltage drives—Part II: Performance assessment,” *IEEE Trans. Power Electron.*, vol. 37, no. 12, pp. 14 237–14 251, Dec. 2022.

[7] S. Kouro, M. A. Perez, J. Rodríguez, A. M. Llor, and H. A. Young, “Model predictive control: MPC’s role in the evolution of power electronics,” *IEEE Ind. Electron. Mag.*, vol. 9, no. 4, pp. 8–21, Dec. 2015.

[8] S. Vazquez, J. Rodríguez, M. Rivera, L. G. Franquelo, and M. Norambuena, “Model predictive control for power converters and drives: Advances and trends,” *IEEE Trans. Ind. Electron.*, vol. 64, no. 2, pp. 935–947, Feb. 2017.

[9] G. S. Buja, “Optimum output waveforms in PWM inverters,” *IEEE Trans. Ind. Appl.*, vol. IA-16, no. 6, pp. 830–836, Nov./Dec. 1980.

[10] T. Geyer and N. Oikonomou, “Model predictive pulse pattern control with very fast transient responses,” in *Proc. IEEE Energy Convers. Congr. Expo.*, Pittsburgh, PA, USA, Sep. 2014, pp. 5518–5524.

[11] J. Rodríguez and P. Cortés, *Predictive control of power converters and electrical drives*. Chichester, UK: Wiley, 2012.

[12] J. Holtz and B. Beyer, “Fast current trajectory tracking control based on synchronous optimal pulsewidth modulation,” *IEEE Trans. Ind. Appl.*, vol. 31, no. 5, pp. 1110–1120, Sep./Oct. 1995.

[13] J. Holtz, “Pulsewidth modulation for electronic power conversion,” *Proc. IEEE*, vol. 82, no. 8, pp. 1194–1214, Aug. 1994.